

A MODEL FOR THE VERTICAL SUBSURFACE RADON TRANSPORT IN "GEOGAS" MICROBUBBLES

András VÁRHEGYI*, István BARANYI* and György SOMOGYI**

Based on the phenomenon of "geogas", rising in the form of microbubbles from deeper regions, the authors have developed a new model for the transport of radon released from deep sources, and a new method for its detection. The advantage of the new model compared to the earlier ones is the elimination of the well-known problems of the radon emanation research methods (penetration depth, reproducibility, etc.), and it provides a qualitative and quantitative description of the transport mechanism, which is realistic from both geological and physical viewpoints. The authors emphasize the role of groundwater and gases of deep origin in the movement of radon, briefly discussing possible sources of these gases. The problems of detecting the radon below the water-table with track detectors are reviewed and the connection between the rock physical parameters (tortuosity, porosity, grain size distribution) and transport characteristics is investigated in detail. Assuming different geological conditions and rock physical parameters theoretical vertical radon concentration and track production profiles were calculated. Finally detectability of deep radon sources depending on geological conditions is analysed and methodological recommendations are made for the more efficient use of the radon emanation uranium exploration methods.

Keywords: radon, transport, models, uranium ores, emanation method, track-etch method, microbubbles, geogas

1. Introduction

A worldwide trend in the exploration for uranium is the growing interest in mineralization at greater depths, after having discovered the near-surface deposits. Methods based on the measurement of gamma radiation (gamma level mapping and gamma spectrometry) are being replaced by other indirect methods like radon emanometry and geochemistry. There is a large volume of literature dealing with the versatile application of the radon emanation (briefly radon) exploration method (detection of uranium ores, prediction of earthquakes, exploration of geothermal energy resources, etc.). The state of the art is well reflected by the review paper of GINGRICH [1984], indicating some of the problems and doubts in the course of development of geochemical exploration using radon.

Results obtained by pump-type emanometers applying short-term sampling are not reliable, the anomaly pattern changes in time. GINGRICH and FISHER [1976] listed eight environmental factors that might influence the instantaneous radon concentration of the soil air. It is rather difficult or impossible

* Mecsek Ore Mining Enterprise, POB 121, Pécs, H-7614

** Institute of Nuclear Research of the Hungarian Academy of Sciences, Debrecen, H-4001
Manuscript received: 26 March, 1986

to take all these effects into account. According to our experience the radon concentration of the soil air can change by one or two orders of magnitude even within the same day.

The 70's brought significant changes in the radon detection devices developed for integrating measurements, first of all the alpha sensitive solid state track detectors have appeared. Using these monitors the undesirable effects caused by short-term variations in the radon concentration of the soil air can be eliminated, although even these integrating measurements indicate long-term seasonal variations. Emanation measurement with inverted cups placed in 50 to 100 cm deep holes is widespread [GINGRICH and FISHER 1976; FLEISCHER and MOGRO-CAMPERO 1978; SOMOGYI et al. 1978; TITOV et al. 1985].

2. Problems of integrating radon measurement techniques

The opinion of scientists involved in uranium exploration is not unanimous concerning the usefulness and reliability of the emanation method, although most of the technical problems encountered in practice have been properly solved. The misting over of detector films [LIKES et al. 1977], the radon – thoron discrimination [WARD et al. 1977], the distinguishing between deep and shallow radon sources [FLEISCHER and MOGRO-CAMPERO 1978], the depth dependence of radon detection [SOMOGYI et al. 1982; KRISTIANSOON and MALMQVIST 1984], the effect of the detector cup geometry and the detector type [FLEISCHER and MOGRO-CAMPERO 1978; SOMOGYI et al. 1982, 1983], the role of the meteorological factors [CLEMETS and WILKENING 1974]: all have been thoroughly studied and are mostly solved problems.

The behaviour of radon in the real physical environment determined by geology, however, raises further specific difficulties. The question of measurement reproducibility in time has not been solved satisfactorily. The reasons for interpretation problems are the seasonal variation in radon emission [SOMOGYI et al. 1978, 1982], and on the other hand the great differences often observed in field measurements carried out close to each other [KRISTIANSOON and MALMQVIST 1984]. These allow only probability conclusions to be reached in the interpretation of the results.

The most severe problem is, however, to determine the maximum depth of Rn sources that can produce concentrations detectable on the surface and significantly higher than the "background noise". Several case histories have been published about the detection of uranium mineralizations at the depth of 100 m or even deeper, using integrating radon measurement [GINGRICH 1975; BECK and GINGRICH 1976; GINGRICH and FISCHER 1976; FLEISCHER and MOGRO-CAMPERO 1978; TITOV et al. 1985]. At the same time under unfavourable geological conditions even near-surface deposits might remain undetected by emanation exploration methods.

In the author's opinion the problems about the emanation method are seated in the lack of a geological and physical model which properly describes

the migration of radon from greater depths to near the surface. No unambiguous exploration criteria are available for planning the technical parameters of emanation measurements and the results cannot be interpreted quantitatively. In the present paper after briefly summarizing the existing theories for radon transport the authors introduce a novel transport mechanism which seems to be able to solve the long-standing problems. Formulas suitable for the quantitative description of the subsurface radon transport and results obtained by the track detector exploration technique are presented as well. Vertical radon concentration profiles calculated using the new theory are shown and some practical methods are recommended.

3. Traditional theories for radon transport

The steady state depth (1D) distribution of radon concentration in a homogeneous host medium is given by the differential equation [GRAMMAKOV 1936]

$$D \frac{\partial^2 c}{\partial z^2} - \frac{\partial(vc)}{\partial z} - \lambda c + Q = 0, \quad (1)$$

where

c is the radon concentration ($\text{atom} \cdot \text{cm}^{-3}$)

D is the diffusion coefficient of radon ($\text{cm}^2 \text{ s}^{-1}$)

v is the velocity of the medium carrying the radon in z direction (cm s^{-1})

λ is the decay constant of radon (s^{-1})

Q is the intensity of radon generation in the host medium ($\text{atom} \cdot \text{cm}^{-3} \cdot \text{s}^{-1}$)

It is noted that in porous media (e.g. in rocks) effective values should be used, like $D = D_{eff}/\varepsilon$ and $v = v_{eff}/\varepsilon$, where ε is the effective porosity of the medium.

Using a wide variety of approximations and boundary conditions different solutions of equation (1) are given in the literature. Solutions of the equation for two simple geological models are summarized in *Tables 1/a* and *b*.

If the transport of radon is due to diffusion only, attenuation of radon concentration moving away from the radon source is described by the diffusion length

$$z_d = \sqrt{D/\lambda} \quad (2)$$

and at this distance the Rn concentration is the e -th part of that at the source. So using the possible highest diffusion coefficient (which is the diffusion coefficient of radon for air: $\sim 0.1 \text{ cm}^2 \cdot \text{s}^{-1}$), the radon concentration decreases to its one thousandth part within 15 m from the source.

To explain the radon movement from greater depths encountered under natural conditions several authors suggest another transport mechanism, the

vertical upward flow of the medium filling the pore space. Detectable radon concentration anomalies from about 100 m deep sources, however, could be explained this way only if a flow velocity of several $\text{m} \cdot \text{day}^{-1}$ is supposed for the medium filling the pores. In our opinion flow velocities of this order of magnitude for the pore filling medium (being either gas or fluid) cannot be taken as realistic ones from the geological viewpoint (excluding some extreme cases, like active faults, volcanic or postvolcanic areas).

According to recent investigations [KRISTIANSSON and MALMQVIST 1982; MALMQVIST and KRISTIANSSON 1984, 1985; BARANYI et al. 1985; SOMOGYI and LÉNÁRT 1985] it seems reasonable that the buoyant force, the result of the differences in the density of ground water and gases moving upward, can ensure the required transport velocities if the upward flow means movement of microbubbles consisting of different gases, including radon. The assumption of upward bubble movement adds new geological, physical and mathematical aspects to the radon transport model.

4. Origin of subsurface gases and their role in radon transport

KRISTIANSSON and MALMQVIST [1982] were the first to suggest that the upward flow of gases from deep sources in bubble form could be a factor of decisive importance in radon transport. In a recent paper the same authors [MALMQVIST and KRISTIANSSON 1984] reported on the measurement of the flux of the upward moving gas bubbles from deep sources ("geogas") under different geologic conditions, and on the chemical composition of these gases.

BARANYI et al. [1985] called the attention to the fact that — especially in the vicinity of radioactive ore deposits — large volumes of gases could be released by radioiysis as well. If the medium is water-bearing a part of the radioactive energy, first of all energy released by alpha decay, is used for decomposition of the water molecules in the close vicinity. According to VOVK [1981] an alpha decay occurring in water can result in $4\text{--}8.5 \cdot 10^3$ radiolytically decomposed water molecules, depending on the energy of the alpha particle. Thus a radioactive ore deposit could be regarded as a special gas-generating object. During the complete decay of a ^{238}U atom, besides the gaseous products of the decay series, one ^{222}Rn and eight ^4He atoms, 36,000 water molecules could be decomposed radiolytically in water-bearing environment, as an average. The released hydrogen generally forms free H_2 molecules, while the oxygen is usually bonded to organic materials often accompanying the uranium deposits or it is released as CO_2 .

Several measurements demonstrate the wide range of possibilities for the existence of an upward gas flow in nature the flux of which may exceed the value of several thousand $\text{cm}^3 \cdot \text{m}^{-2} \cdot \text{year}^{-1}$ [VOYTOV 1974, SUGISAKI et al. 1983, MALMQVIST and KRISTIANSSON 1984]. In case of such a significant gas flow through water-filled rock pores, movement of gases in the form of microbubbles and the development of an unusually high vertical component of the gas flow

Table I/a

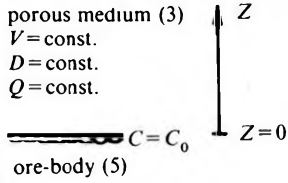
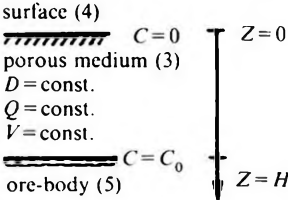
Model I: "thick" overburden (1)	Model II: "shallow" overburden (2)
porous medium (3) $V = \text{const.}$ $D = \text{const.}$ $Q = \text{const.}$  ore-body (5)	surface (4)  ore-body (5)
Boundary conditions: (6) at $Z=0$ $C = C_0$ when $Z \rightarrow \infty$ $C = \frac{Q}{\lambda}$	Boundary conditions: (6) at $Z=0$ $C = 0$ at $Z=H$ $C = C_0$

Table I/b

(8) Mechanism	(9) Differential equation	(10) General solution	(11) Solution for Model I.	(12) Solution for Model II.
(1) decay + generation	$-\lambda c + Q = 0$	$c = \frac{Q}{\lambda}$	$c = \frac{Q}{\lambda}$ boundary conditions cannot be used (13)	$c = \frac{Q}{\lambda}$ boundary conditions cannot be used (13)
(2) diffusion + decay	$D \frac{\partial^2 c}{\partial Z^2} - \lambda c = 0$	$c = K_1 e^{\sqrt{\frac{\lambda}{D}} Z} + K_2 e^{-\sqrt{\frac{\lambda}{D}} Z}$	$c = c_0 e^{-\sqrt{\frac{\lambda}{D}} Z}$	$c = c_0 \frac{\text{sh} \sqrt{\frac{\lambda}{D}} Z}{\text{sh} \sqrt{\frac{\lambda}{D}} H}$
(3) transport + decay	$-v \frac{\partial c}{\partial Z} - \lambda c = 0$	$c = K e^{-\frac{\lambda}{v} Z}$	$c = c_0 e^{-\frac{\lambda}{v} Z}$	$c = c_0 e^{\frac{\lambda}{v} (Z-H)}$ only the lower boundary condition can be used (14)
(4) diffusion + decay + generation	$D \frac{\partial^2 c}{\partial Z^2} - \lambda c + Q = 0$	$c = K_1 e^{\sqrt{\frac{\lambda}{D}} Z} + K_2 e^{-\sqrt{\frac{\lambda}{D}} Z} + \frac{Q}{\lambda}$	$c = \left(c_0 - \frac{Q}{\lambda} \right) e^{-\sqrt{\frac{\lambda}{D}} Z} + \frac{Q}{\lambda}$	$c = \left(c_0 - \frac{Q}{\lambda} \right) \frac{\text{sh} \sqrt{\frac{\lambda}{D}} Z}{\text{sh} \sqrt{\frac{\lambda}{D}} H} + \frac{Q}{\lambda} \left(1 - \frac{\text{sh} \sqrt{\frac{\lambda}{D}} (H-Z)}{\text{sh} \sqrt{\frac{\lambda}{D}} H} \right)$
(5) transport + decay + generation	$-v \frac{\partial c}{\partial Z} - \lambda c + Q = 0$	$c = K e^{-\frac{\lambda}{v} Z} + \frac{Q}{\lambda}$	$c = \left(c_0 - \frac{Q}{\lambda} \right) e^{-\frac{\lambda}{v} Z} + \frac{Q}{\lambda}$	$c = \left(c_0 - \frac{Q}{\lambda} \right) e^{\frac{\lambda}{v} (Z-H)} + \frac{Q}{\lambda}$ only the lower boundary condition can be used (14)
(6) diffusion + transport + decay	$D \frac{\partial^2 c}{\partial Z^2} - v \frac{\partial c}{\partial Z} - \lambda c = 0$	$c = e^{\frac{v}{2D} Z} \left[K_1 \exp Z \sqrt{\frac{v^2}{4D^2} + \frac{\lambda}{D}} + K_2 \exp \left(-Z \sqrt{\frac{v^2}{4D^2} + \frac{\lambda}{D}} \right) \right]$	$c = c_0 \exp \left[\frac{v}{2D} - \sqrt{\frac{v^2}{4D^2} + \frac{\lambda}{D}} \right] Z$	$c = c_0 e^{\frac{v}{2D} (H-Z)} \frac{\text{sh} Z \sqrt{\frac{v^2}{4D^2} + \frac{\lambda}{D}}}{\text{sh} H \sqrt{\frac{v^2}{4D^2} + \frac{\lambda}{D}}}$
(7) diffusion + transport + decay + generation	$D \frac{\partial^2 c}{\partial Z^2} - v \frac{\partial c}{\partial Z} - \lambda c + Q = 0$	$c = e^{\frac{v}{2D} Z} \left[K_1 \exp Z \sqrt{\frac{v^2}{4D^2} + \frac{\lambda}{D}} + K_2 \exp \left(-Z \sqrt{\frac{v^2}{4D^2} + \frac{\lambda}{D}} \right) \right] + \frac{Q}{\lambda}$	$c = \left(c_0 - \frac{Q}{\lambda} \right) \exp \left[\frac{v}{2D} - \sqrt{\frac{v^2}{4D^2} + \frac{\lambda}{D}} \right] Z + \frac{Q}{\lambda}$	$c = e^{\frac{v}{2D} (H-Z)} \left(c_0 - \frac{Q}{\lambda} \right) \frac{\text{sh} Z \sqrt{\frac{v^2}{4D^2} + \frac{\lambda}{D}}}{\text{sh} H \sqrt{\frac{v^2}{4D^2} + \frac{\lambda}{D}}} + \frac{Q}{\lambda} \left(1 - e^{-\frac{v}{2D} Z} \frac{\text{sh} (H-Z) \sqrt{\frac{v^2}{4D^2} + \frac{\lambda}{D}}}{\text{sh} H \sqrt{\frac{v^2}{4D^2} + \frac{\lambda}{D}}} \right)$

Table 1/a. Main data and boundary conditions for the idealized radon transport models of Table 1/b

Table 1/b. Solutions for the differential equations describing the radon transport for the two models of Table 1/a. Equilibrium in time and the presence and absence of different physical mechanisms are assumed, $c(z)$ is the vertical profile of radon concentration for the boundary conditions of the given models; K , K_1 and K_2 are constants

1/a. táblázat. Az 1/b. táblázatban használt, idealizált radon-szállítás modellek jellemző adatai és határfeltételei

1 — I. Modell: „vastag” fedő; 2 — II. Modell: „vékony” fedő; 3 — porózus közeg; 4 — felszín; 5 — érctest; 6 — határfeltételek

1/b. táblázat. A radon-transzportot leíró differenciálegyenlet megoldásai az 1/a. táblázatban vázolt két modell esetén, időbeli egyensúlyt és különböző fizikai mechanizmusok jelenlétét, ill. hiányát feltételezve. $c(z)$: a radonkoncentráció mélységprofilja az adott modellek határfeltételei között; K , K_1 és K_2 : állandók

1 — bomlás + keletkezés; 2 — diffúzió + bomlás; 3 — szállítás + bomlás;
4 — diffúzió + bomlás + keletkezés; 5 — szállítás + bomlás + keletkezés;
6 — diffúzió + szállítás + bomlás; 7 — diffúzió + szállítás + bomlás + keletkezés;
8 — Mechanizmus; 9 — Differenciál egyenlet; 10 — Általános megoldás;
11 — I. Modell szerinti megoldás; 12 — II. Modell szerinti megoldás;
13 — határfeltétel nem vehető figyelembe; 14 — csak az alsó határfeltétel vehető figyelembe

Табл. 1/a. Характерные данные и граничные условия моделей переноса радона, примененных в табл. 1/b

1 — Модель I. «мощные» наносы; 2 — Модель II «маломощные» наносы; 3 — пористая среда; 4 — дневная поверхность; 5 — руда; 6 — граничные условия

Табл. 1/b. Решения дифференциального уравнения переноса радона для моделей табл. 1/a. предполагая наличие временного равновесия при наличии и отсутствии разных физических процессов

1 — распад + образование; 2 — диффузия + распад; 3 — перенос + распад; 4 — диффузия + распад + образование; 5 — перенос + распад + образование; 6 — диффузия + перенос + распад; 7 — диффузия + перенос + распад + образование; 8 — процесс; 9 — дифференц. уравнение; 10 — общее решение; 11 — решение по модели I.; 12 — решение по модели II.; 13 — граничное условие нельзя учитывать; 14 — учитывается лишь нижнее граничное условие

velocity should be supposed. Gas bubbles passing through the water saturated uranium ore deposit and those produced by radiolysis could carry away a part of the released radon [KRISTIANSSON and MALMQVIST 1982], and could ensure the rapid transport (with total time comparable to the half-life of radon) up to the uppermost level of the continuous pore water system, the ground-water table. From the viewpoint of radon monitoring this bubble transport mechanism provides favourable conditions only if there is no geological formation (e.g. clay layer) impermeable to water or gases between the ore deposit and the water table.

The medium above the water table behaves in a different way in radon transport, the buoyant force result of specific weight differences between the gases and the pore fluid ceases to exist, and the movement of radon is determined by physical laws governing the behaviour of gases filling the pore space in a solid medium. From among the pore gas components the radon has the highest relative atomic mass, therefore in this zone the lighter components of the geogas (H_2 , He) might have a higher mobility. Above the water table the diffusion can be regarded as the basic mechanism in upward movement of the radon. In what follows we make an attempt to give a quantitative description of the radon movement in a medium below and above the water table, assuming two different transport mechanisms, viz. microbubbles and diffusion.

5. Physical model for radon transport in microbubbles

The velocity of the microbubble movement in water is determined by the Stokes' law

$$v = \frac{g}{18\eta_w} (\rho_w - \rho_g)d^2 \tag{3}$$

- where g is acceleration due to gravity (cms^{-2})
- η_w is dynamic viscosity of water ($\text{gcm}^{-1}\text{s}^{-1}$)
- ρ_w is density of water (gcm^{-3})
- ρ_g is density of the gas in the bubbles (gcm^{-3})
- d is diameter of the spherical gas bubble (cm).

The velocity in the differential equation (1) describing the radon transport should be substituted for velocity given by Eq. (3). As the velocity is a function of depth (i.e. the coordinate z) too, this equation has no trivial solution. Namely during their upward movement the bubbles are expanding because the hydrostatic pressure is decreasing, thus the bubble velocity is increasing according to Eq. (3).

Using Boyle's gas law ($p \cdot V = \text{constant}$ at a given temperature), and the equation giving the hydrostatic pressure ($p = p_0 + \rho_w g z$)

$$v = v_0 \left(\frac{h_0}{h_0 + z} \right)^{2/3} \tag{4}$$

is obtained for the velocity of the bubbles as a function of depth, where v_0 is the velocity of the bubble at the moment of reaching the water surface (i.e. the highest value of transport velocity), h_0 is the piezometric height of a water column being in hydrostatic equilibrium with atmospheric pressure p_0 (practically 10 m). The equation is valid only in water; in rocks the velocity might be significantly lower (see Section 9).

In first approximation the terms describing the diffusion and the radon production (Q) can be neglected in Eq. (1). The validity of this assumption has already been checked for the first term [VÁRHEGYI et al. 1986], and neglecting the source term Q which describes the local radon generation does not effect basically the essentials of the solution (the solution including the term Q is discussed elsewhere [BARANYI et al. 1985]. In this case the general solution of Eq. (1) is

$$c = K(h_0 + z)^{2/3} \cdot \exp \left[\frac{3h_0\lambda}{5v_0} \left(\frac{h_0 + z}{h_0} \right)^{5/3} \right] \quad (5)$$

It is noted that z is positive downward and $z=0$ at the water table. For negative z values this equation is meaningless because above the water table the diffusion is considered to be the basic physical process of radon transport, and here the general solution of the transport equation is (see Table I)

$$c = K_1 \exp(z\sqrt{\lambda/D}) + K_2 \exp(-z\sqrt{\lambda/D}) \quad (6)$$

K , K_1 and K_2 in Eqs. (5) and (6) are arbitrary constants.

6. The depth function of radon concentration

For quantitative description of the radon transport the rock volume between the ore deposit and the surface is divided into two regions: from the ore-body up to the water table, where the pores are filled with water (medium 2), and the region between the water table and the surface without continuous water saturation (medium 1). Parameters of the model are shown in *Figure 1*. The depth change of radon concentration (radon profile) in medium 1 is given by Eq. (6), while in medium 2 by Eq. (5). Using the relevant boundary conditions we get for the radon profile in medium 1

$$c = c_0 \frac{\text{sh}(z\sqrt{\lambda/D})}{\text{sh}(h\sqrt{\lambda/D})} \quad (7)$$

and in medium 2

$$c = c_s \left(\frac{y}{y_s} \right)^{2/3} \exp \left[\frac{3h_0\lambda}{5v_0} (y^{5/3} - y_s^{5/3}) \right] \quad (8)$$

where

$$y = \frac{h_0 + z - h}{h_0} \quad \text{and} \quad y_s = \frac{h_0 + H - h}{h_0} \quad (8a)$$

If we suppose that c_0 at the water table ($z = h$) is independent of the approach direction, i.e. the same value could be obtained in media 1 and 2 (this is not trivial), then for c_0 we get

$$c_0 = c_s y_s^{-2/3} \cdot \exp \left[\frac{3h_0 \lambda}{5v_0} (1 - y_s^{5/3}) \right] \quad (9)$$

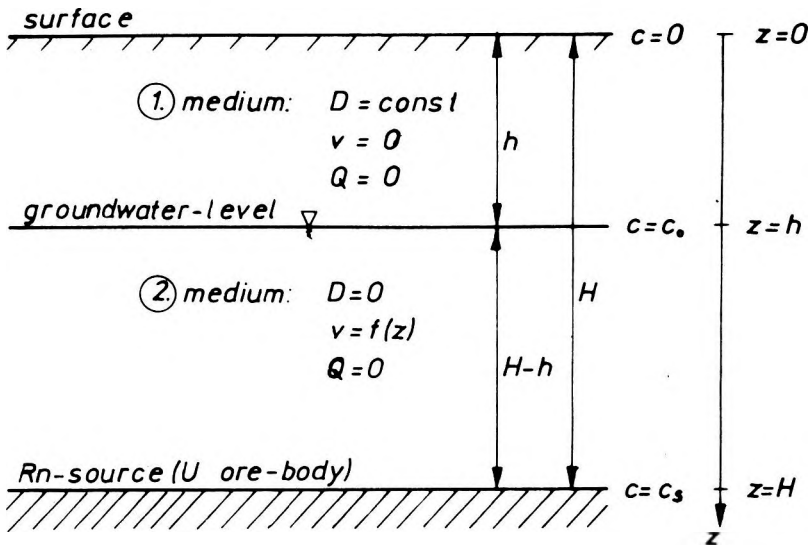


Fig. 1. Parameters used in model calculations for vertical one-dimensional radon transport in microbubbles and by diffusion

1. ábra. A mikrobuborékos és diffúziós, vertikális, egydimenziós radontranszport-modell számításaink során használt paramétereit

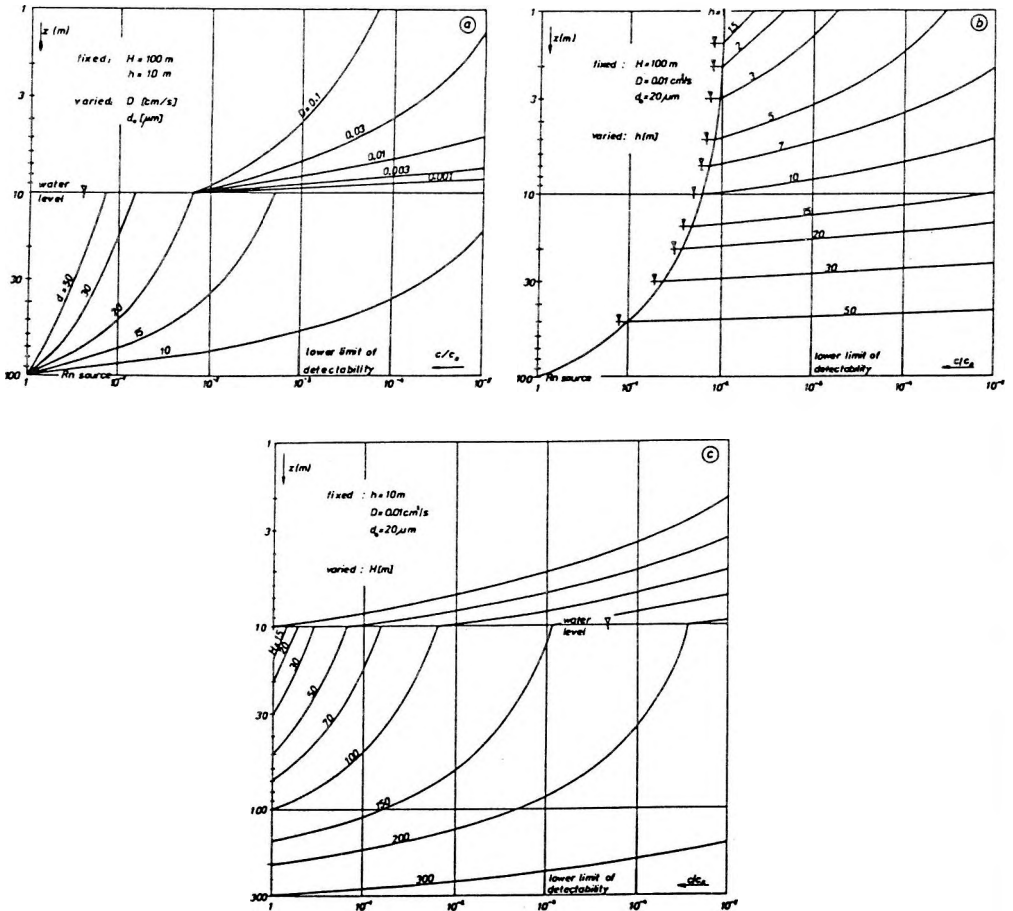
Рис. 1. Параметры, используемые нами при расчетах микропузырьковой и диффузионной моделей вертикального, одномерного переноса радона

7. Theoretical radon profiles

Theoretical profiles of the relative radon concentration c/c_s can be calculated using equations (7) to (9) for any value of D , v_0 (or using Stokes' law for the maximum bubble diameter d_0), h and H .

Of course, this form of the curves (without including the rock physical parameters) can reflect only the trend of the expected real changes. They are, however, suitable for drawing some important—sometimes unexpected and surprising—conclusions. In *Figure 2* theoretical relative radon concentration profiles are shown calculated for some arbitrarily fixed values of the parameters. In the figure the concentration range considered as practical detectability threshold (minimum of signal-to-noise ratio required) is marked. This range is determined by the radon concentrations always present in the vicinity of the monitoring site (background).

Figure 2a shows the radon profiles for different d_0 and D values if the ore-body is at the depth of 100 m and the water table at 10 m. The most striking feature of the figure is that the attenuation in the radon concentration does not exceed three orders of magnitude for bubble diameters over 15 μm if the whole 90 m below the water table is considered (because the radon being in the bubbles



relatively quickly reaches the water table). Above this level, however, up to the depth of 1 m below the surface (which is the depth generally applied in traditional track detector measurements) there is a further attenuation of more than two orders of magnitude in the radon concentration, even under the most favourable conditions.

Figure 2b shows the effect of the water table depth on the radon profile for 100 m source depth. A practically important conclusion is that for water tables deeper than a few m there is a significant attenuation in the near-surface radon concentration. At the same time in case of shallow water tables anomalous radon concentrations can be detected from deep sources with an attenuation of less than two orders of magnitude in the concentration compared to that at the source. Attempts were made to explain the temporal changes in radon concentration obtained in field measurements by the development of global subsurface flows; these attempts, however, failed in identifying the real cause of this phenomenon. A consequence of our model is that the assumption of such a mechanism is not mandatory, the phenomenon can be explained by changes in the water table.

Figure 2c shows the effect of the depth to the ore-body on the radon profile for a water table at 10 m. It can be seen that for the given parameters an anomalous radon concentration can be detected at the water table even if the source depth exceeds 150 m. Near to the surface, however, there is no chance to detect deep sources.

Fig. 2. Theoretical curves of vertical radon transport in microbubbles and by diffusion

- a) Attenuation of the relative radon concentration (c/c_s) for a source at the depth of 100 m, if the water table is at 10 m. d_0 — bubble diameter at the water table; D — diffusion coefficient of radon for medium 1; c_s — radon concentration at the source
- b) The effect of the depth to the water table (h) on the vertical radon concentration profile, assuming a maximum bubble diameter d_0 of 20 μm
- c) The effect of the source depth (H) on the vertical radon concentration profile, assuming a maximum bubble diameter of 20 μm

2. ábra. A mikrobuborékos és diffúziós, vertikális radontranszport elméleti görbéi

- a) A relatív radonkoncentráció (c/c_s) változása egy 100 m mélyen levő forrás felett, ha a talajvízszint 10 m mélyen van. d_0 — buborékátmérő a vízszintnél; D — a radon diffúziós állandója a vízszint feletti közegben; c_s — radonkoncentráció a forrásnál
- b) A talajvízszint (h) változásának hatása a mélységi radonkoncentráció-profilra, 20 μm -es maximális buborékátmérőt (d_0) feltételezve
- c) A forrásmélység (H) hatása a mélységi radonkoncentráció-profilra, 20 μm -es maximális buborékátmérőt feltételezve

Рис. 2. Теоретические кривые микропузырькового и диффузионного, вертикального переноса радона

- a) Изменение относительной концентрации радона (c/c_s) над источником на глубине 100 м при залегании уровня грунтовой воды на глубине 10 м. d_0 — диаметр пузыря на уровне воды; D — постоянная диффузии радона в среде над уровнем воды; c_s — концентрация радона у источника
- b) влияние изменения уровня грунтовой воды (h) на профиль глубинной концентрации радона при предположении максимального диаметра пузыря, равного 20 мкм (d_0)
- c) влияние глубины источника (H) на профиль глубинной концентрации радона при предположении максимального диаметра пузыря, равного 20 мкм

8. Theoretical track production profiles for radon measurements with track detectors

Theoretical vertical concentration profiles from the ore-body up to the water table have been shown for radon carried by "geogas" bubbles for different boundary conditions. Using the track detector radon measuring technique, however, the track production is not proportional to the radon content because of the pressure changes in the cup placed into the water. The pressure in the sensitive volume of the cup is obviously in equilibrium with the sum of the actual hydrostatic (p) and atmospheric pressures. Consequently the track production efficiency of the detector changes according to

$$\frac{R}{R_s} = \frac{p_s}{p} = \frac{h_0 + H - h}{h_0 + z - h} \quad (10)$$

because of the pressure dependence of the range of alpha particles in air (R). The relationship between the measured track density and the radon concentration is

$$\frac{Q}{Q_s} = \frac{P_s}{p} \cdot \frac{c}{c_s} \quad (11)$$

Finally, using Eqs. (11) and (8), the theoretical track density profile for the configuration of Figure 1 is

$$\frac{Q}{Q_s} = \left(\frac{y}{y_s}\right)^{-1/3} \exp\left[\frac{3h_0\lambda}{5v_0}(y^{5/3} - y_s^{5/3})\right] \quad (12)$$

One of the remarkable features of Eq. (12) is that it has a minimum at a depth of z_{min} if certain boundary conditions are met. The minimum can be found at the depth of

$$z_{min} = h + h_0 \left[\left(\frac{v_0}{3h_0\lambda} \right)^{3/5} - 1 \right] \quad (13)$$

below the surface.

This equation is valid only between h and H . If $v_0 \leq 0.23 \text{ mh}^{-1}$ no minimum might be expected. We have observed a minimum in the track density profile measured in a 270 m deep borehole [SOMOGYI and LÉNÁRT 1985].

Figure 3a shows a typical set of track density profiles calculated using equation (12) and assuming different bubble diameters at the water table. It is worth mentioning that for fixed initial conditions (water depth, bubble size) the track density profiles depend on water temperature through viscosity as well. Results of calculations about this phenomenon are shown in Figure 3b. It is obvious from the figure that our model results in higher radon concentrations at the surface of thermal springs.

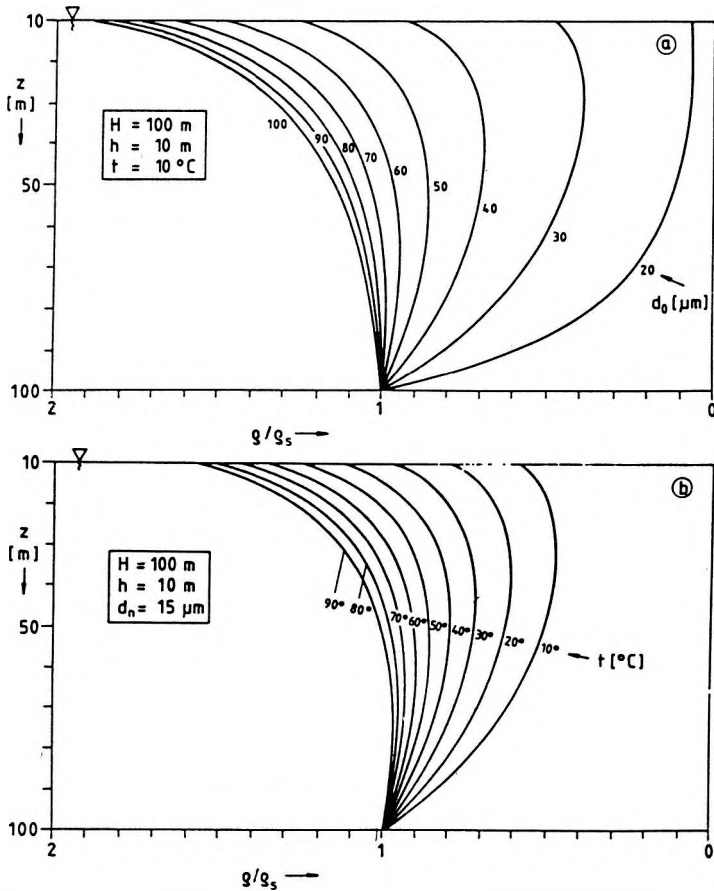


Fig. 3. Theoretical track density (q/q_s) – depth (z) profiles below the water table for an alpha-sensitive track detector and for vertical radon transport in microbubbles
 a) assuming “geogas” bubbles of different diameter and a water temperature of 10 °C
 b) as a function of water temperature, if the initial diameter of “geogas” bubbles is identical (15 μ m)

3. ábra. Alfa-részecskékre érzékeny nukleáris nyomdetektorral mérhető relatív nyomsűrűség (q/q_s) elméletileg várható változása a vízszint alatt mért mélység függvényében, mikrobuborékos, vertikális radontranszport esetén

- a) Különböző átmérőjű „geogáz” buborékokat és 10 °C-os vizet feltételezve
- b) Különböző hőmérsékletű vizekben, ha a „geogáz” mikrobuborékok kezdeti átmérője azonos (15 μ m)

Рис. 3. Теоретически ожидаемое изменение относительной плотности следов (q/q_s), измеряемых при помощи чувствительного к α -частицам ядерного детектора в зависимости от глубины под уровнем воды при микропузырькового вертикального переноса радона
 а) при предположении пузырей «геогаза» с различными диаметрами и температуры воды, равной 10 °C
 б) в водах при различных температурах при одинаковом исходном диаметре микропузырьков «геогаза» (15 мкм)

9. Role of petrophysical parameters in radon transport

In order to describe the radon transport in microbubbles under realistic geological conditions using Eqs. (7) to (9) some connection should be found between the variables in the equations and the rock physical parameters. Because of the significant spatial changes in the rock physical parameters this connection could be a trend only, established by statistical approach. In this way, however, it is possible to determine clearly the direction and measure of the effects of the individual rock properties on the radon transport. Rock physical parameters can be introduced into the equations describing the radon transport through the diffusion coefficient D , the concentration at the source c_s , and the maximum bubble velocity v_0 (or using Stokes' law through the maximum bubble diameter d_0). The role of D and c_s is not dealt with in the present paper, these topics have already been thoroughly and widely discussed in the literature [e.g. TANNER 1964]. In what follows we make some comments of conceptual importance only concerning the connection between the rock structure and bubble velocity.

9.1 Role of tortuosity and porosity

In our description of the radon transport the diameter of the microbubbles d and their upward flow velocity v have been connected in first approximation by Stokes' law (3). The Stokes' law, however, in this form applies only to the flow of bubbles in a fluid, and therefore it cannot take into account that in rocks this flow might occur along forced trajectories only, namely through the inter-connected fissure and pore system of rocks. The sinuosity of actual flow paths in rocks is expressed by the rock physical parameter of tortuosity (t). Using the tortuosity the upward component of the bubble velocity is given by

$$v_{\uparrow} \leq \frac{v}{t^2}. \quad (14)$$

It should be noted, however, that because of the narrowing of the flow paths at several places and adhesion forces between the pore wall and the bubble some of the bubbles might get stuck for longer times, their flow might slow down or they might be disintegrated into smaller bubbles. These effects might cause a further significant decrease in the resulting velocity. Therefore a wide distribution of velocities should be visualized, where Eq. (14) gives the upper limit of velocities only.

The vertical bubble velocity can be expressed by the porosity ε , which can be measured more easily than t . For loose sediments the relation between the tortuosity and porosity is given by a simplified form of Archie's formula

$$t^2 \cong \frac{1}{\sqrt{\varepsilon}} \quad (15)$$

Thus the vertical velocity component can be related to that obtained by using Stokes' law by

$$v_{\uparrow} \leq \sqrt{\varepsilon} \cdot v. \quad (16)$$

9.2 Role of grain size distribution

There is a parameter of more or less unknown value in Stokes' velocity function, the bubble diameter. The maximum value of that is somehow related to the texture of the rock. It is obvious that the narrowest cross section of the pore paths provides an upper limit for the bubble diameter. In fractured rocks (where the bulk of pore volume consists of an interconnected system of fractures and fissures, e.g. in fault zones) the size of the bubbles is determined supposedly by the minimum spatial dimension of the interconnected fracture system.

For porous rocks consisting of grains (e.g. sand, sandstone) an idealized model of the matrix structure should be used in the theoretical investigation of this question. Let us suppose an equigranular grain size distribution, i.e. it might be characterized by a single parameter, by grain diameter D_m (D_m may be called mean grain size as well). For this case the two extreme states, the possible loosest and most dense fills are shown in *Figure 4*. The real case might be somewhere between these two extremes. Anyway, the two limits of the largest bubbles that can pass through the grains and the two concrete values of rock porosity shown in *Figure 4* can be assigned to these two extreme cases [EGERER 1977]. Taking the origin of the ε - d coordinate system as a third point to the previously mentioned two points (obviously, if there is no porosity there are no bubbles) a parabola can be fitted arbitrarily to these three points which is described by

$$d = 1.26 D_m \varepsilon (\varepsilon + 0.21). \quad (17)$$

Using equations (16) and (17), and the Stokes' formula (3) — accepting the idealized conditions and other assumptions — a relationship could have been derived between the velocity v_0 in Eq. (8) describing the radon transport, and rock physical parameters. After all, for porous water-saturated rocks the bubble velocity (or its maximum value) could be traced back to two simple rock properties, the porosity and the mean grain diameter D_m :

$$v_0 \leq 0.088 \frac{g}{\eta_w} (\rho_w - \rho_g) \varepsilon^{5/2} (\varepsilon + 0.21)^2 D_m^2 \quad (18)$$

Two comments should be made on equation (18):

- (1) The velocity determined this way should be considered only as a maximum value, because of the reasons mentioned above. Only the "most lucky" bubbles may gain this velocity, but these might carry the bulk of the radon.
- (2) We have investigated the effect of the mean grain diameter D_m only for equigranular grain distribution, and this can be found only rarely in nature. The relation between D_m and the actual grain size distribution is very

difficult to investigate theoretically. It is probable, however, that in case of a wide grain size distribution D_m is shifted towards the finer grain sizes (the space between the larger grains is filled in with the smaller ones, thus the cross section available for bubble flow is reduced).

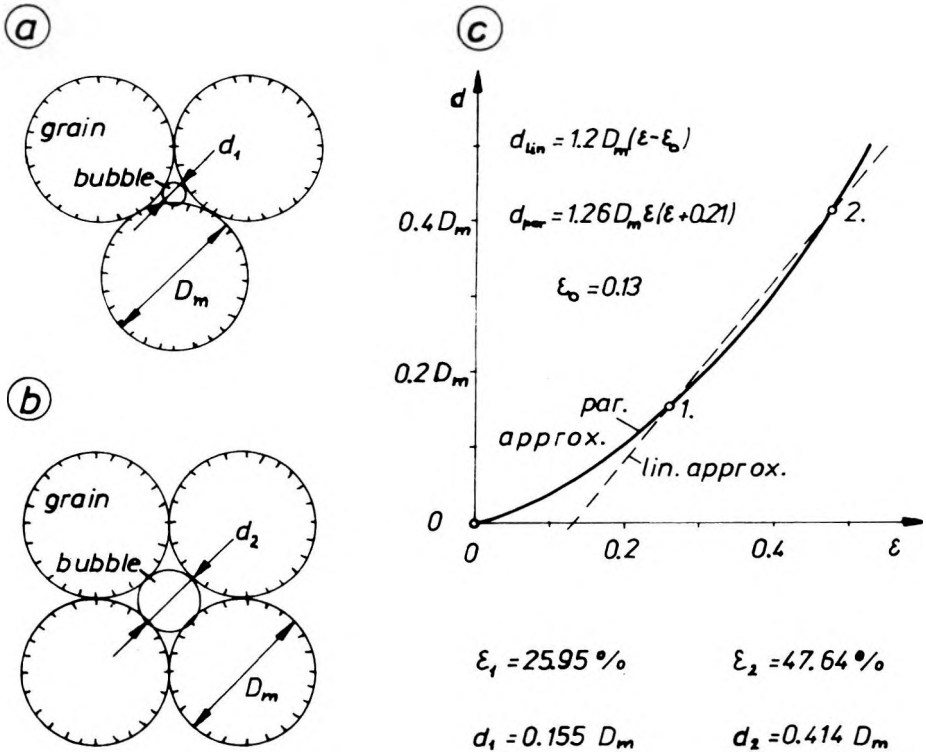


Fig. 4. The relationship between the possible maximum bubble diameter (d) and rock porosity (ϵ) for

- a) the most dense; b) the loosest fill, assuming an equigranular grain size (D_m) distribution;
- c) parabolic approximation of the $d(\epsilon)$ function

4. ábra. A lehetséges maximális buborékátmérő (d) és a kőzetporozitás (ϵ) kapcsolata a legszorosabb és b) leglazább szemcseilleszkedésnél, ekvigranuláris szemcseméret (D_m)-eloszlást feltételezve; c) a $d(\epsilon)$ függvény parabolikus közelítése

Рис. 4. Связь между максимальным диаметром пузыря (d) и пористостью породы (ϵ) при самом плотном а) и самом рыхлом б) прилегании зерн при предположении эквигранулярной зернистости (D_m); в) аппроксимация функции $d(\epsilon)$ параболой

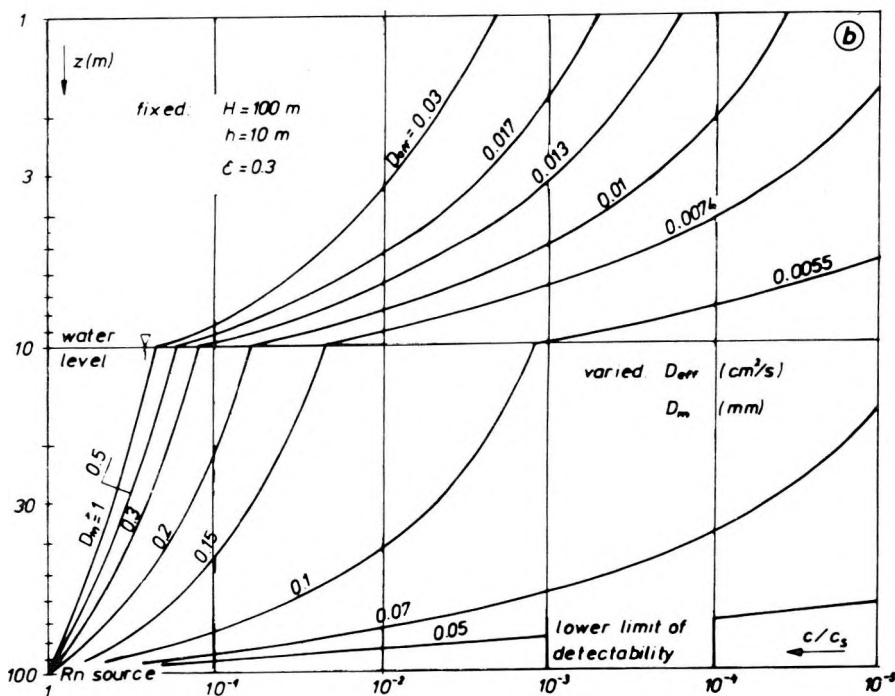
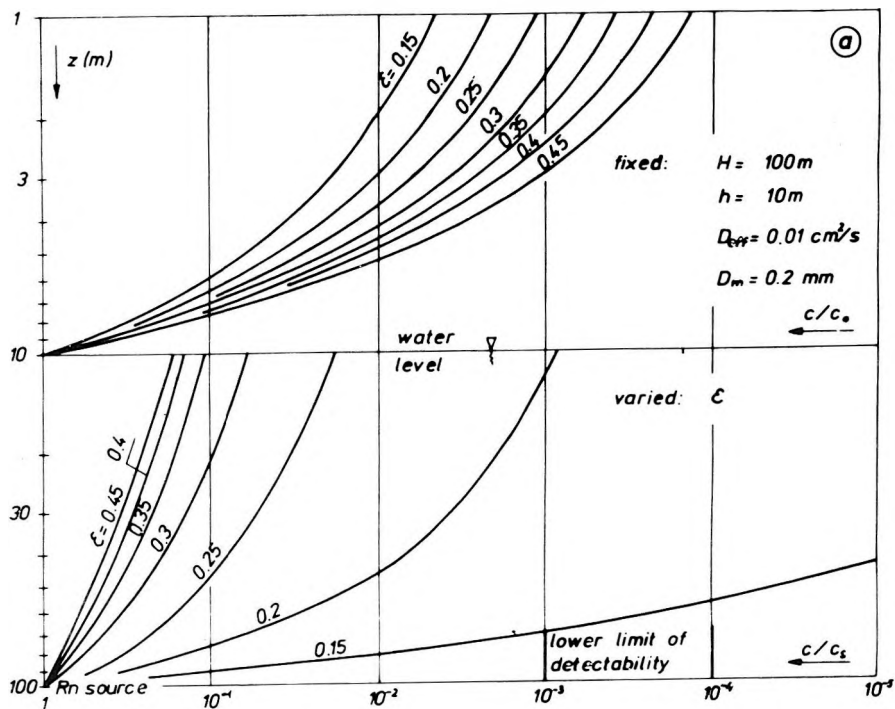
10. Theoretical radon profiles in porous rocks

The concentration profile calculated using equations (8) and (18) is shown in *Figure 5*. Here only the water saturated rock region (below the water table) is discussed.

The effect of rock porosity on the radon profile can be studied in *Figure 5/a*. In calculation of the curve set the following parameters were fixed: depth to the ore-body below the water table is 100 m; the mean grain diameter is 0.2 mm. It can be seen clearly that the radon profile is practically insensitive to variations in porosity for the given parameters and for porosities over 35%. For porosities lower than 20%, however, the radon concentration significantly attenuates with distance from the source.

Figure 5/b shows the effect of the grain mean diameter D_m on the radon profile (fixed parameters: $H = 100$ m, $\varepsilon = 0.3$) For grain diameters above 1 mm variations in D_m have no effect on the radon profile (this includes the extreme case of $D_m \rightarrow \infty$, i.e. the medium is water alone, if there is no other factor reducing the bubble size). It can be seen that down to $D_m = 0.2$ mm the decrease in the grain diameter does not effect significantly the radon concentration. Any further decrease in D_m , however, dramatically reduces the radon transport.

Based on the diagrams shown it seems that — assuming a radon transport in microbubbles — there is no practical possibility for detection of radon concentration anomalies due to deep sources if the overburden has a low effective porosity ($\varepsilon < 20\%$) and/or a small mean grain diameter ($D_m < 0.1$ mm) (e.g. mud, silt, clay, loess, etc.). Exceptions are the cases when other favourable properties of the rock structure (vertical fracturing, fault zone, etc.) provide other channels for radon transport. In porous ($\varepsilon > 25\%$) rocks of coarse grain size ($D_m > 0.2$ mm) and/or in rocks with macrofractures, along fractured and water saturated fault zones — at least at or near to the water table — the chances for detecting deep radon sources are excellent.



11. Practical recommendations

No doubt, coincidence of several favourable geological conditions is required for effective operation of radon transport in microbubbles from the viewpoint of uranium exploration. The presence of a high enough geogas flux and water saturated, loose porous rocks and the absence of layers impermeable to gases are all prerequisites. In favourable cases, however, mineralizations at depths of a few hundred meters can be detected by radon measurements, as has been demonstrated by several case histories.

According to our model calculations the radon, as one of the components of geogas flowing upward in microbubbles, reaches the water table at relatively high velocity. Its further movement towards the surface is, however, controlled by the "slow" diffusion. Therefore when the water table is at depths of several meters below the surface, detectors traditionally placed near to the surface cannot detect the radon from deep sources (Figure 2). Nevertheless, using shallow drill holes the radon monitors might be placed near to the water table and the detectability of deep radon sources could be improved by several orders of magnitude. The increase in exploration costs and a better chance for detecting deeper mineralizations are factors of opposite effect and an optimum should be found by strategical considerations.

The authors have developed a research technology and exploration tools based on the transport theory described. This technology has been routinely applied in uranium exploration in Hungary since 1983. BARANYI et al. [1985] have also published some practical results in addition to an experiment directly demonstrating the validity of the "geogas" bubble model [SOMOGYI and LÉNÁRT 1985].

Fig. 5. A theoretical approach to the connection between the vertical radon transport in microbubbles and petrophysical parameters, assuming a porous rock matrix consisting of grains.

- a) Effect of effective rock porosity (ϵ) on radon concentration profiles
- b) Effect of the mean grain size (D_m) on radon concentration profiles

5. ábra. A mikrobuborékos, vertikális radontranszport és a kőzetfizikai paraméterek kapcsolatának elméleti megközelítése, szemcsés-porózus kőzetstruktúrát feltételezve.

- a) A kőzetek effektív porozitásának (ϵ) hatása a radonkoncentráció-profilra
- b) A kőzetek mértékadó szemcseátmérőjének (D_m) hatása a radonkoncentráció-profilra

Рис. 5. Теоретическая аппроксимация связи микропузырькового вертикального переноса радона с физическими параметрами пород при предположении зернисто-пористой структуры породы

- a) влияние эффективной пористости (ϵ) пород на профиль концентрации радона
- b) влияние преобладающего диаметра зерн (D_m) пород на профиль концентрации радона

REFERENCES

- BARANYI I., GERZSON I., VÁRHEGYI A. 1985: A new hypothesis of radon migration and its practical application in the emanation exploration method of uranium occurrences (in Hungarian). *Magyar Geofizika*, **26**, 5–6, pp. 226–232
- BECK L. S., GINGRICH J. E. 1976: Track etch orientation survey in the Cluff lake area, Northern Saskatchewan. *CIM. Bulletin*, **69**, pp. 104–109
- CLEMENTS W. E., WILKENING M. H. 1974: Atmospheric pressure effects on Rn-222 transport across the earth-air interface. *J. Geophys. Res.*, **79**, 33, pp. 5025–5029
- EGERER F. 1977: Physics of rocks (in Hungarian). Tankönyvkiadó. Budapest, 224 p.
- FLEISCHER R. L., MOGRO-CAMPERO A. 1978: Mapping of integrated radon emanation for detection of long-distance migration of gases within the earth: Techniques and principles. *J. Geophys. Res.*, **83**, B7, pp. 3539–3549
- GINGRICH J. E. 1975: Results from a new uranium exploration method. *Transaction of SME.*, **258**, pp. 61–64
- GINGRICH J. E. 1984: Radon as a geochemical exploration tool. *J. Geochem. Explor.*, **21**, 1, pp. 19–39
- GINGRICH J. E., FISHER J. C. 1976: Uranium exploration using the track-etch method. *IAEA-SM-208/19*, pp. 213–224
- GRAMMAKOV A. G. 1936: On the influence of some factors in the spreading of radioactive emanations under natural conditions (in Russian). *Zhur. Geofiziki*, **6**, pp. 123–148
- KRISTIANSSON K., MALMQVIST L. 1982: Evidence for nondiffusive transport of $^{222}_{86}\text{Rn}$ in the ground and a new physical model for the transport. *Geophysics*, **47**, 10, pp. 1444–1452
- KRISTIANSSON K., MALMQVIST L. 1984: The depth-dependence of the concentration of $^{222}_{86}\text{Rn}$ in soil gas near the surface and its implication for exploration. *Geoexploration*, **22**, pp. 17–41
- LIKES R. S., MOGRO-CAMPERO A., FLEISCHER R. L. 1979: Moisture-intensive monitoring of radon. *Nucl. Instr. Meth.*, **159**, 2–3, pp. 395–400
- MALMQVIST L., KRISTIANSSON K. 1984: Experimental evidence for an ascending microflow of geogas in the ground. *Earth Planet. Sci. Lett.*, **70**, 2, pp. 407–416
- MALMQVIST L., KRISTIANSSON K. 1985: A physical mechanism for the release of free gases in the lithosphere. *Geoexploration*, **23**, 4, pp. 447–453
- SOMOGYI GY., MEDVECZKY L., VARGA Zs., GERZSON I., VADOS I. 1978: Field macroradiography measuring radon exhalation. *Isotopenpraxis*, **14**, 10, pp. 343–347
- SOMOGYI GY., NÉMETH G., PÁLFAI J., GERZSON I. 1982: Subsurface radon-distribution measurements with LR-115, CR-39 and TL-detectors. *Solid State Nucl. Track Det.*, Proc. 11th. Int. Conf., Bristol, 1981., P. H. Fowler and V. M. Clapham eds., Pergamon Press, pp. 525–529
- SOMOGYI GY., VARGA Zs., PARIPÁS B. 1983: Measurement of radon, radon daughters and thoron concentrations by multi-detector devices. *The Nucleus*, **20**, pp. 51–55
- SOMOGYI GY., LÉNÁRT L. 1985: Time-integrated radon measurements in spring and well waters by track technique. Presented at 13th Int. Conf. on Solid State Nucl. Track Det., Rome, 23–27. Sept. 1985
- SUGISAKI R., IDO M., TAKEDA H., ISOBE Y., HAYASHI Y., NAKAMURA M., SATAKE H., MIZUTANI Y. 1983: Origin of hydrogen and carbon dioxide in fault gases and its relation to fault activity. *J. Geol.*, **91**, pp. 239–258
- TANNER A. B. 1964: Radon migration in the ground — a review. *The Natural Radiation Environment*, J. A. S. Adams and W. M. Lowder eds., University of Chicago Press, pp. 161–190
- TITOV V. K., VENKOV V. A., AVDEEVA T. L., KUVSHYNNIKOVA E. J. 1985: Expositional emanation methods for exploration of mineral resources (in Russian). *Nedra, Leningrad*, 132 p.
- VÁRHEGYI A., BARANYI I., SOMOGYI GY. 1986: A model for the subsurface vertical transport of radon carried by geogas microbubbles (in Hungarian). *Izotóptechnika*, **29**, pp. 73–104
- VOYTOV G. I. 1974: Evaluation of the intensity of gas-exchange on shield terrains (some examples from the Ukrainian shield) (in Russian). *Geol. Zs.*, **34**, 2, pp. 78–85
- VOVK I. F. 1981: Radiolitic model for the composition of solutions in the crystalline basement of shields (in Russian). *Geokhimiya*, **26**, pp. 467–480
- WARD W. J., III., FLEISCHER R. L., MOGRO-CAMPERO A. 1977: Barrier technique for separate measurement of radon isotopes. *Rev. Sci. Instrum.*, **48**, 11, pp. 1440–1441

GEOGÁZ MIKROBUBORÉKOK SEGÍTSÉGÉVEL MEGVALÓSULÓ FELSZÍNALATTI, VERTIKÁLIS RADON-SZÁLLÍTÁS MODELLJE

VÁRHEGYI András, BARANYI István és SOMOGYI György

A nagy mélységekből mikrobuborékok formájában feláramló „geogáz” jelenségére alapozva a szerzők a mélységi forrásból származó radon szállításának és kimutatásának egy új modelljét dolgozták ki. Az új modell előnye az eddigiekkel szemben, hogy segítségével feloldhatók az emanációs kutatómódszer ismert problémái (lehatolási mélység, reprodukálhatóság stb.), és a szállítási mechanizmusra földtani-fizikai szempontból reális, kvalitatív és kvantitatív leírást ad. A szerzők kiemelik a felszínalatti vizek és a mélyben keletkező gázok szerepét a radon migrációjában, röviden utalva utóbbiak lehetséges eredetére. Áttekintik a vízszint alatti nyomdetektoros radonkimutatás problémáit, és részletesen megvizsgálják egyes közetfizikai paraméterek (tortuozitás, porozitás, szemcseméret-eloszlás) és a szállítási jellemzők kapcsolatát. Különböző földtani körülmények és közetfizikai paraméterek feltételezésével elméleti úton számított mélységi radonkoncentráció és nyomdetektoros alfa-nyomsűrűség szelvényeket mutatnak be. Végül elemzik, hogy milyen földtani körülmények esetén van esély nagy mélységű radonforrás kimutatására, és új módszertani ajánlásokat tesznek az emanációs urán kutatómódszer hatékonyabb alkalmazására.

МОДЕЛЬ ПОДЗЕМНОГО ВЕРТИКАЛЬНОГО ПЕРЕНОСА РАДОНА, ОСУЩЕСТВЛЯЕМОГО С ПОМОЩЬЮ МИКРОПУЗЫРЕЙ ГЕОГАЗА

Андраш ВАРХЕДИ, Иштван БАРАНИ и Дёрдь ШОМОДИ

Авторами разработана новая модель переноса и детектирования радона, образовавшегося из глубоких источников, на основании явления «геогаза», поднимающегося с больших глубин в виде микропузырей. Достоинство новой модели заключается в том, что с его применением исчезают известные проблемы эманационного способа (глубинность исследования, повторяемость и др.) а модель переноса дает с геолого-геофизической точки зрения реальное качественное и количественное описание процессов. Авторами подчеркивается роль в миграции радона подземных вод и образовавшихся в глубине газов, с краткой ссылкой на их возможную генетику. Рассматриваются проблемы детектирования радона под уровнем воды, и детально изучается связь между характеристиками переноса и петрофизическими параметрами (извилистость, пористость, распределение размеров зерн). Показаны рассчитанные глубинное содержание радона и профили густоты альфа-следов при предположении разных геологических обстановок и петрофизических параметров. Анализируется, что при какой геологической обстановке имеется возможность детектировать глубинные источники радона, даются новые методические рекомендации для повышения эффективности эманационного поиска урана.

